Acta Crystallographica Section F
Structural Biology and Crystallization Communications
ISSN 1744-3091

Crystallization and preliminary crystallographic studies of *Helicobacter pylori* arginase

Jinyong Zhang,[a] Xiaoli Zhang,[a] Xuhu Mao,[a] Quanming Zou[a]* and Defeng Li[b]*

[a]Department of Clinical Microbiology and Immunology, College of Medical Laboratory Science, Third Military Medical University, Chongqing 400038, People's Republic of China, and [b]National Laboratory of Biomacromolecules, Institute of Biophysics, Chinese Academy of Sciences, 15 Datun Road, Beijing 100101, People's Republic of China

Correspondence e-mail: qmzou2007@163.com, lidefeng@moon.ibp.ac.cn

Received 15 December 2010
Accepted 15 April 2011

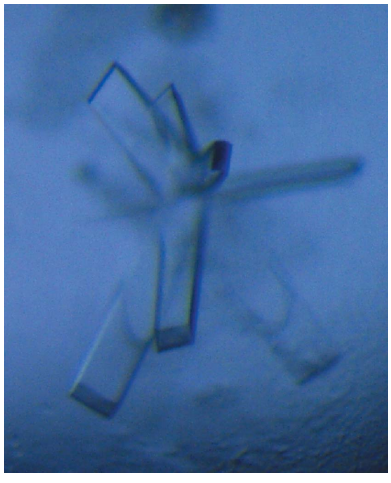

Helicobacter pylori arginase is an important factor in evasion of the host's immune system and contributes to persistent infection by this bacterium. It is unique in many aspects compared with other arginases: for example, it has optimal activity with Co^{2+} as a cofactor rather than Mn^{2+} and has strongest activity at acidic pH instead of alkaline pH. In this study, *H. pylori* arginase was purified and crystallized in complex with Mn^{2+} and a diffraction data set was collected to 2.2 Å resolution. The crystals belonged to space group $P2_12_12_1$, with unit-cell parameters a = 94.69, b = 102.24, c = 148.61 Å.

1. Introduction

Helicobacter pylori infects more than 50% of the world population; it is the cause of gastritis and peptic ulcers and a risk factor for gastric cancer (Kusters *et al.*, 2006). It usually persists for the life of the host and is not eradicated despite a vigorous immune response (Suerbaum & Michetti, 2002). The persistent infection by this bacterium results from immune evasion by several effectors, such as the virulence factors CagA and VacA (Cooke *et al.*, 2005). Arginase is another protein that has recently been identified to show immunosuppressant properties and is probably involved in the bacterium's evasion of the host's immune system (Baldari *et al.*, 2005). It is a urea-cycle enzyme that catalyzes the hydrolysis of arginine to yield ornithine and urea (Muszyńska *et al.*, 1972) and is present in almost all known life forms, playing a crucial role in nitrogen metabolism. *H. pylori* arginase competes with host inducible nitric oxide synthase for the common substrate L-arginine; this reduces the synthesis of NO, an important component of innate immunity and an effective antimicrobial agent that is able to kill invading pathogens directly (Bussière *et al.*, 2005). Additionally, *H. pylori* arginase is able to inhibit human T-cell proliferation and T-cell CD3ζ expression and thus efficiently reduces the host cellular immune response (Zabaleta *et al.*, 2004). Also, its product urea is utilized by urease to generate ammonia and carbon dioxide, which helps to neutralize the acidic environment of the stomach and thus facilitate colonization by the bacterium (McGee *et al.*, 1999).

Two arginase isozymes have been identified in eukaryotes: arginase I and II. The former is highly expressed in liver and plays a key role in the urea cycle, while the latter is a mitochondrial enzyme that is involved in L-arginine homeostasis (Kepka-Lenhart *et al.*, 2008). Arginases from many bacteria have also been identified, such as those from *Bacillus caldovelox* (Bewley *et al.*, 1999) and *Streptomyces clavuligerus* (Elkins *et al.*, 2002). The activity and catalytic mechanism of arginases from eukaryotes and some bacteria have been well characterized. These enzymes show highest activity in the presence of manganese and have an optimum pH of 9.0–11.0 (Jenkinson *et al.*, 1996; Bussière *et al.*, 2005; Kanyo *et al.*, 1996). However, *H. pylori* arginase is only distantly related to arginases of known structure (28% sequence identity to the closest homologue *B. caldovelox* arginase; PDB entry 1cev; Bewley *et al.*, 1999) and is unique in the following aspects. (i) It shows optimal activity with Co^{2+} as a cofactor rather than Mn^{2+} (McGee *et al.*, 2004). (ii) It shows strongest activity at acidic pH (pH 6.1) instead of alkaline pH (McGee *et al.*, 2004),

Table 1
Statistics of *H. pylori* arginase diffraction data.

Values in parentheses are for the highest resolution shell.

Space group	$P2_12_12_1$
Unit-cell parameters	a = 94.69, b = 102.24, c = 148.61
Wavelength (Å)	1.0000
Resolution (Å)	34.92–2.20 (2.32–2.20)
No. of reflections	73842
$R_{\rm merge}$†	10.1 (31.2)
Multiplicity	6.8 (6.4)
Mean $I/\sigma(I)$	11.3 (4.8)
Completeness (%)	99.9 (99.9)

† $R_{\rm merge} = \sum_{hkl}\sum_i |I_i(hkl) - \langle I(hkl)\rangle| / \sum_{hkl}\sum_i I_i(hkl)$, where $\langle I(hkl)\rangle$ is the mean of the observations $I_i(hkl)$ of reflection hkl.

which may be an adaptation to the acidic colonization environment of *H. pylori*. (iii) It contains an insertion corresponding to residues 153–165 which was not found in other arginases and which has been proposed to interact with the membrane since this enzyme is cell-envelope associated (Mendz *et al.*, 1998). (iv) It is extremely sensitive to reducing agents such as dithiothreitol and β-mercaptoethanol and its activity can be inhibited by small doses of reducing agent (McGee *et al.*, 2004). (v) It has been identified to exist as a monomer in solution (work to be published), in contrast to typical trimeric or hexameric (Bewley *et al.*, 1999) complexes, although a human arginase has been reported to be active as a monomer (Aguirre & Kasche, 1983).

To identify the role of *H. pylori* in infection and study its unique biochemical and enzymatic properties, we intend to determine the structure and enzymatic mechanism of *H. pylori* arginase. Here, we report the crystallization, diffraction data collection and preliminary crystallographic studies of arginase from *H. pylori*.

2. Materials and methods

2.1. Cloning, expression and purification

The *rocF* gene (NCBI Gene ID 899897) encoding *H. pylori* arginase was amplified from the genome of *H. pylori* 26695 and cloned into an expression vector derived from the pET-22b(+) plasmid (Novagen) and placed between *Nde*I and *Xho*I restriction sites. The *H. pylori* arginase C-terminus was fused to a His_6 tag (LEHHHHHH) in order to facilitate purification. The insert was sequenced and found to be in complete agreement with the expected sequence.

Escherichia coli BL21 (DE3) pLysS strain (Invitrogen) transformed with plasmid pET22b-*rocF* was grown at 310 K in 2 l Luria–Bertani medium supplemented with ampicillin (100 mg ml^{-1}) until the optical density at 600 nm (OD_{600}) reached 0.6. Isopropyl β-D-1-thiogalactopyranoside (IPTG) was then added to a final concentration of 1 m*M* to induce expression of the recombinant protein. Cell growth was continued at 310 K for 3 h. The cells were harvested by centrifugation and the bacterial pellets were resuspended in lysis buffer (20 m*M* phosphate buffer pH 8.0, 300 m*M* NaCl and 10 m*M* imidazole) and disrupted by ultrasonication. Insoluble cellular material was removed by centrifugation. The supernatant was loaded onto a nickel–nitrilotriacetic acid agarose (Ni–NTA; Novagen) column previously equilibrated with lysis buffer. The column was washed with wash buffer (20 m*M* phosphate buffer pH 8.0, 300 m*M* NaCl and 20 m*M* imidazole). His-tagged *H. pylori* RocF was then eluted using washing buffer (20 m*M* phosphate buffer pH 8.0, 300 m*M* NaCl and 250 m*M* imidazole). The eluted protein was concentrated to about 1 ml by ultrafiltration (Millipore) and loaded onto a Superdex 200 HiLoad 16/60 column (GE Healthcare) previously equilibrated with 20 m*M* Tris–HCl pH 7.5, 150 m*M* NaCl. The peak corresponding to the *H. pylori* arginase monomer was collected; the protein was concentrated to about 80 mg ml^{-1} and stored at 277 K for further crystallization experiments. Protein concentrations were determined from the absorbance at 280 nm, assuming an A_{280} of 0.543 for a 1.0 mg ml^{-1} solution.

2.2. Crystallization

Initial crystallization screening for the *H. pylori* arginase used Crystal Screen, Index, PEG/Ion and PEG/Ion 2 from Hampton Research. Crystallization experiments were set up *via* the hanging-drop vapour-diffusion technique at 293 K. Each drop was formed by mixing equal volumes (1 µl) of protein solution (80 mg ml^{-1} arginase in 20 m*M* Tris–HCl pH 7.5, 150 m*M* NaCl) and reservoir solution and was allowed to equilibrate against 420 µl reservoir solution. Conditions giving positive hits were optimized by varying the type and the concentration of precipitants, salts, buffers, organic compounds and additives (Additive Screen, Hampton Research).

2.3. Data collection and processing

Prior to data collection, the *H. pylori* arginase crystals were briefly soaked (for about 15 s) in cryoprotectant, which corresponded to the mother liquor with the addition of 15%(*v*/*v*) glycerol. Crystals were then mounted for X-ray data collection using CryoLoops (Hampton Research) and flash-cooled in a nitrogen-gas stream at 95 K. A native data set to 2.2 Å resolution was collected at a wavelength of 1.0000 Å on beamline 17U of the Shanghai Synchrotron Radiation Facility using a CCD detector. We collected 180 images with 1° oscillation per image. *MOSFLM* (v.7.0.4; Leslie, 2006) and *SCALA* (v.6.0) from the *CCP*4 program suite (v.6.0.2; Winn *et al.*, 2011) were used for indexing, integration and scaling of the diffraction data set.

3. Results

Crystals were initially obtained from Hampton Research Index screen condition No. 65 [0.1 *M* ammonium acetate, 0.1 *M* Bis-Tris pH 5.5, 17%(*w*/*v*) PEG 10 000] and PEG/Ion screen condition No. 3 [0.2 *M* ammonium fluoride, 20%(*w*/*v*) PEG 3350 pH 6.2]. The opti-

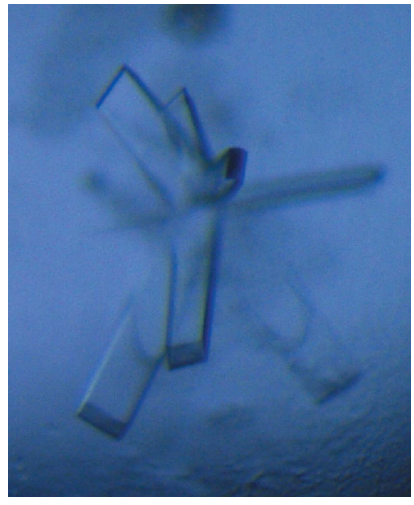

Figure 1
H. pylori arginase crystals grown using the hanging-drop method in 25% PEG 3350, 100 m*M* Bis-Tris pH 5.5, 1 m*M* $MnCl_2$, 15 m*M* guanidine hydrochloride. Dimensions are 0.5 × 0.1 × 0.06 mm.

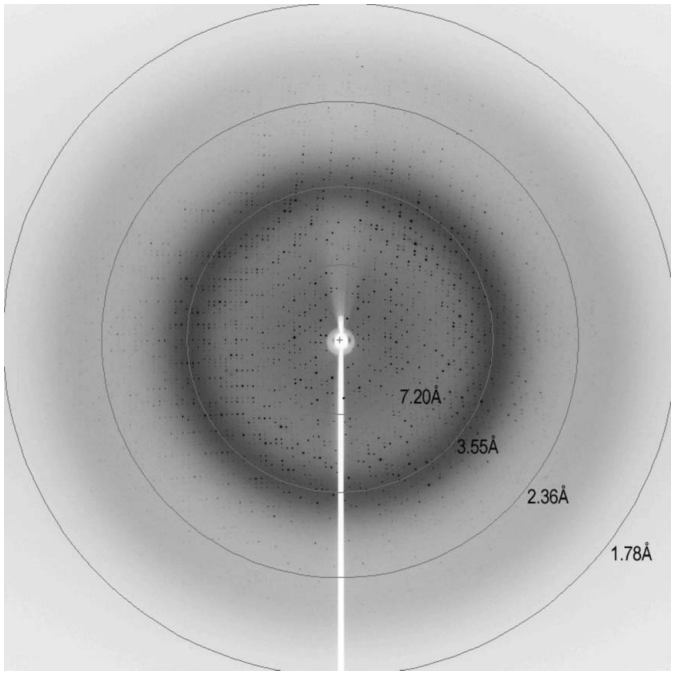

Figure 2
A typical diffraction pattern of an *H. pylori* arginase crystal.

mized crystallization condition consisted of 25% polyethylene glycol 3350, 100 m*M* Bis-Tris pH 5.5, 1 m*M* $MnCl_2$, 15 m*M* guanidine hydrochloride using hanging-drop vapour diffusion; equal volumes (1 µl) of protein solution and reservoir solution and 0.3 µl 30%(*w*/*v*) 1,5-diaminopentane were mixed at room temperature. Crystals appeared overnight and grew to dimensions of about 0.5 × 0.1 × 0.06 mm in a few days (Fig. 1). Data-collection statistics for the native crystal are shown in Table 1. The crystal diffracted to a resolution of 2.2 Å and belonged to space group $P2_12_12_1$, with unit-cell parameters a = 94.69, b = 102.24, c = 148.61 Å (Fig. 2).

There are probably 3–5 *H. pylori* arginase molecules per asymmetric unit, with corresponding Matthews coefficients of 3.33, 2.50 and 2.00 $Å^3\ Da^{-1}$ and solvent contents of 63.1, 50.8 and 38.5%, respectively. Self-rotation functions calculated by *MOLREP* in the *CCP*4 program suite (v.6.0.2; Winn *et al.*, 2011) at various resolutions showed neither threefold, fourfold, fivefold nor sixfold noncrystallographic symmetry axes; however, perpendicular twofold noncrystallographic symmetry axes close to crystallographic symmetry axes were observed. Thus, we propose that there are four molecules with 222 point-group symmetry in the asymmetric unit.

The high quality of the data forms a solid foundation for our structural studies. Attempts to solve the phase problem by molecular replacement using existing models such as PDB entries 1d3v (Cox *et al.*, 1999) and 1cev (Bewley *et al.*, 1999) were not successful and this work is still in progress.

The authors are grateful to the Photon Factory (KEK, Tsukuba, Japan) and the Shanghai Synchrotron Radiation Facility for providing access to synchrotron-radiation facilities for X-ray diffraction experiments. This work was supported by funding from the National Science Foundation of China (31000336).

References

Aguirre, R. & Kasche, V. (1983). *Eur. J. Biochem.* **130**, 373–381.
Baldari, C. T., Lanzavecchia, A. & Telford, J. L. (2005). *Trends Immunol.* **126**, 199–207.
Bewley, M. C., Jeffrey, P. D., Patchett, M. L., Kanyo, Z. F. & Baker, E. N. (1999). *Structure*, **7**, 435–448.
Bussière, F. I., Chaturvedi, R., Cheng, Y., Gobert, A. P., Asim, M., Blumberg, D. R., Xu, H., Kim, P. Y., Hacker, A., Casero, R. A. & Wilson, K. T. (2005). *J. Biol. Chem.* **280**, 2409–2412.
Cooke, C. L., Huff, J. L. & Solnick, J. V. (2005). *FEMS Immunol. Med. Microbiol.* **45**, 11–23.
Cox, J. D., Kim, N. N., Traish, A. M. & Christianson, D. W. (1999). *Nature Struct. Biol.* **6**, 1043–1048.
Elkins, J. M., Clifton, I. J., Hernández, H., Doan, L. X., Robinson, C. V., Schofield, C. J. & Hewitson, K. S. (2002). *Biochem. J.* **366**, 423–434.
Jenkinson, C. P., Grody, W. W. & Cederbaum, S. D. (1996). *Comp. Biochem. Physiol. B Biochem. Mol. Biol.* **114**, 107–132.
Kanyo, Z. F., Scolnick, L. R., Ash, D. E. & Christianson, D. W. (1996). *Nature (London)*, **383**, 554–557.
Kepka-Lenhart, D., Ash, D. E. & Morris, S. M. (2008). *Methods Enzymol.* **440**, 221–230.
Kusters, J. G., van Vliet, A. H. & Kuipers, E. J. (2006). *Clin. Microbiol. Rev.* **19**, 449–490.
Leslie, A. G. W. (2006). *Acta Cryst.* D**62**, 48–57.
McGee, D. J., Radcliff, F. J., Mendz, G. L., Ferrero, R. L. & Mobley, H. L. (1999). *J. Bacteriol.* **181**, 7314–7322.
McGee, D. J., Zabaleta, J., Viator, R. J., Testerman, T. L., Ochoa, A. C. & Mendz, G. L. (2004). *Eur. J. Biochem.* **271**, 1952–1962.
Mendz, G. L., Holmes, E. M. & Ferrero, R. L. (1998). *Biochim. Biophys. Acta*, **1388**, 465–477.
Muszyńska, G., Severina, L. O. & Lobyreva, L. W. (1972). *Acta Biochim. Pol.* **19**, 109–116.
Suerbaum, S. & Michetti, P. (2002). *N. Engl. J. Med.* **347**, 1175–1186.
Winn, M. D. *et al.* (2011). *Acta Cryst.* D**67**, 235–242.
Zabaleta, J., McGee, D. J., Zea, A. H., Hernández, C. P., Rodriguez, P. C., Sierra, R. A., Correa, P. & Ochoa, A. C. (2004). *J. Immunol.* **173**, 586–593.